Steady-State Measurements on the Fructose 6-Phosphate/Fructose 1,6-Bisphosphate Interconversion Cycle

David C. Hauri, Peidong Shen, Adam P. Arkin, and John Ross*

Department of Chemistry, Stanford University, Stanford, California 94305

Received: September 20, 1996; In Final Form: December 27, 1996[⊗]

Steady-state measurements are presented of the concentration of fructose 1,6-bisphosphate (F16BP) in a flow reactor containing the enzymes phosphofructokinase 1, fructose 1,6-bisphosphatase, and creatine kinase, under the regulation of combinations of the regulatory species fructose 2,6-bisphosphate, citrate, glycerol 3-phosphate, and adenosine 5′-monophosphate. We use a recently described capillary electrophoresis protocol for sample analysis, which allows for the simultaneous separation and quantification of many glycolytic species, including isomers. We compare our results to theoretical work on logical properties of biological reaction networks and conclude that the fructose 6-phosphate/fructose 1,6-bisphosphate interconversion cycle can be considered to be a switch in glycolysis: a fuzzy logic aggregation operator.

Introduction

In prior work, we have discussed the implementation of logic gates and sequential, as well as parallel computers, by means of macroscopic chemical kinetics.[1−5] A simple experiment demonstrated a parallel computation of pattern recognition.[6] This work was followed by a theoretical investigation of possible computational functions inherent in biochemical reaction networks in which we showed that relatively simple enzymatic reaction mechanisms may yield logic functions such as AND, OR, and NOR gates.[7] The rational for such studies was stated in that work: "Biochemical reaction networks (BRNs), such as glycolysis and the tricarboxylic acid cycle, are an integral part of the machinery by which an organism maintains itself and adapts to its environment. These networks are responsible for numerous cellular tasks including the maintenance of homeostasis and the creation and propagation of chemical signals such as those indicating hunger or satiation. It is often very difficult to determine the underlying logic of the regulation of even relatively small portions of a BRN. First, the subnetwork may be highly interconnected and contain many feedback loops, branching pathways, etc. Second, it is difficult to determine all the kinetic parameters that determine the behavior of a BRN *in vitro* let alone *in vivo*... Third, the great range of temporal and spatial scales over which a large BRN can react to the perturbation of its variables makes it difficult to deduce the laws of biological control and signal processing from examination of models of the dynamic equations of motion... Therefore, it is desirable to develop additional techniques for the investigation of reaction mechanisms, their control and signal processing." The article concluded with the study of a portion of glycolysis embedded in a large metabolic model which showed the presence of a "fuzzy aggregation operator". This operator has properties similar to that of a fuzzy AND gate that controls the switch from glycolysis to gluconeogenesis in response to signals of low blood glucose and abundant fuel for the tricarboxylic acid cycle (TCA). The Boolean function in biological systems have been studied in refs 8 and 9.

In this article we report experiments on the stationary kinetic states of a small part of glycolysis, the reactions shown in Figure 1. We measure the stationary state concentration of fructose 1,6-bisphosphate (F16BP) as the response to variation in the concentrations of the stimuli inputs of fructose 2,6-bisphosphate (F26BP), citrate, adenosine 5′-monophosphate (AMP), and glycerol 3-phospate (G3P), which we refer to as "effectors". These experiments are compared with calculations and were designed to test, in a simple way, the predictions of the presence of logic functions as discussed in ref 7.

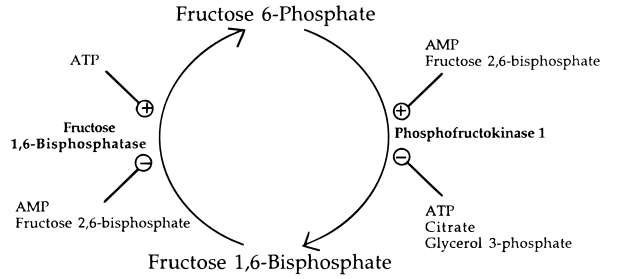

Figure 1. Schematic diagram of the fructose 6-phosphate/fructose 1,6-bisphosphate cycle. Some effectors of the enzymes are noted by lines ending in circles; ⊕, indicates activators and ⊖, indicates inhibitors. Enzymes are noted in boldface type.

Materials and Methods

Chemicals and Enzymes. All chemicals were purchased from Sigma. Reactions were carried out in a solution of 30 mM 4-(2-hydroxyethyl)-1-piperazineethane sulfonic acid (HEPES), 50 mM potassium chloride, 1 mM potassium phosphate, 2 mM dithiothreitol (DTT), 5 mM magnesium chloride, 2 mM adenosine triphosphate (ATP), 2 mM creatine phosphate, and 300 μM F6P, buffered at pH 7.1 with sodium hydroxide, which we will refer to as "enzyme buffer". We prepared enzyme aliquots containing 0.75 units phosphofructokinase 1, 80 units creatine kinase, and 3 mg bovine serum albumin (BSA) in 200 μL enzyme buffer, which we then froze at −80 °C for not less than 24 h and not more than 3 weeks. Enzyme buffer solutions were refrigerated and stored for not more than 10 days.

Flow Reactor. Enzyme buffer was flowed into a 1.17 mL continuous-flow, stirred tank reactor (CSTR) through a peristaltic pump (Model SA 8031 by Ismatec, Zürich, Switzerland) at a rate of 0.20 mL/min. Once inside the CSTR, the solution was stirred with a teflon stirring disk which occupied most of the space inside the vessel. The solution flowed past a 10 000 MW ultrafiltration membrane (YM 10 Diaflo by Amicon,

[⊗] Abstract published in *Advance ACS Abstracts,* April 15, 1997.

S1089-5647(96)02901-X CCC: $14.00 © 1997 American Chemical Society

Beverly, MA) at the top of the reactor, which was permeable to all species present in the basic enzyme buffer, but was not permeable to enzymes or BSA. Thus, the enzymes were confined to the reactor, and their total concentrations did not change over the course of the experiment. The outflow was then collected in a vial and analyzed with capillary zone electrophoresis. All samples were analyzed within 1 h of collection. In order to avoid contamination by enzymes from previous runs, all components of the reactor were washed, soaked in the Terg-A-Zyme detergent solution (Alconox, Inc., NY), and then soaked in doubly distilled water prior to use. After flowing enzyme buffer through the system, we flowed into it a thawed aliquot of the PFK1 mixture and 0.2 units fructose 1,6-bisphosphatase (F16BPase) (except for the citrate and F26BP experiment, where we used 0.15 units F16BPase rather than 0.2 units; this was done to increase the concentration of F16BP so that a significant decrease in its concentration could be observed and errors minimized). The F16BPase was not frozen with the PFK1 because it was less stable to freezing on several trial runs.

Detection and Quantification. We used the detection method developed and previously described by the authors.[10] We analyzed our results on an HP ^{3D}CE system (CE = capillary electrophoresis) (Hewlett-Packard Company, Wilmington, DE) with the built-in photodiode-array detector set at a wavelength of 280 nm. We used a 51 cm fused silica capillary (45 cm effective length) with an internal diameter of 50 μm (320 μm o.d.). Signals were collected and processed on an HP Vectra XM2 4/100i PC computer using ^{3D}CE ChemStation software. The capillary temperature was kept constant at 20 $\pm$ 0.1 °C, and the applied voltage was 20 kV, with the cathode being at the inlet end and the anode at the detector end of the capillary. We injected samples by applying a negative pressure of 0.75 psi for 5 s.

Our flow buffer contained 5.5 mM 4-hydroxybenzoic acid (a chromophore used in indirect UV detection), 0.5 mM tetradecyltrimethylammonium bromide (to reverse the electroosmotic flow) and NaOH to a pH of 11.6.

We flushed new fused silica capillaries successively with 1 M NaOH for 1 h and 0.01 M NaOH for 30 min and running buffer for 40 min. Each day prior to use, we rinsed the capillary with running buffer for at least 40 min at 40 °C, and between runs, we washed it with running buffer for 2 min. In some instances, the running buffer was replenished before each run.

This regimen gives highly reproducible, quantifiable results.

Sample Collection. After flushing the capillary, we make two preliminary electrophoresis runs with the enzyme buffer. We have found that retention times are not stable for the first two runs, so we discard these. For calibration, we then take two measurements of a standard solution with 200 μM F16BP dissolved in enzyme buffer. Finally, we take a measurement of the enzyme buffer flowing out of the CSTR before enzyme has been added, to ensure that no active enzyme remains in the CSTR from a previous run. If there is a measurable F16BP peak, we empty the CSTR, rewash, and begin again with a different membrane while the old one soaks. Samples are run on the CE twice and the results are averaged, unless time constraints during the experiment force only one measurement (about 20% of the samples were run only once).

After adding the enzymes to the CSTR as discussed above, we flow in enzyme buffer for 30 minutes. At a flow rate of 0.20 mL/min, within 30 min over 99% of the original solution in the reactor has been replaced by the inflow solution, and the system is at steady-state (the kinetics of the reaction and effector control are fast compared to this time scale). We have noticed a slow, linear increase in the concentration of F16BP with time, which is probably due to a slow decay of F16BPase, but may have a more complex origin. Due to this change in enzyme activity, we take one sample with no effectors in the enzyme buffer at the start of each experiment and one sample at the end of each experiment. We then use the change in the concentration of F16BP for these samples to construct a linear correction in the measured concentration as a function of time, which we apply to the measurements taken in between. Also because of the change in enzyme activity we run an experiment for a maximum of about 5 h before cleaning the CSTR and replacing the enzyme.

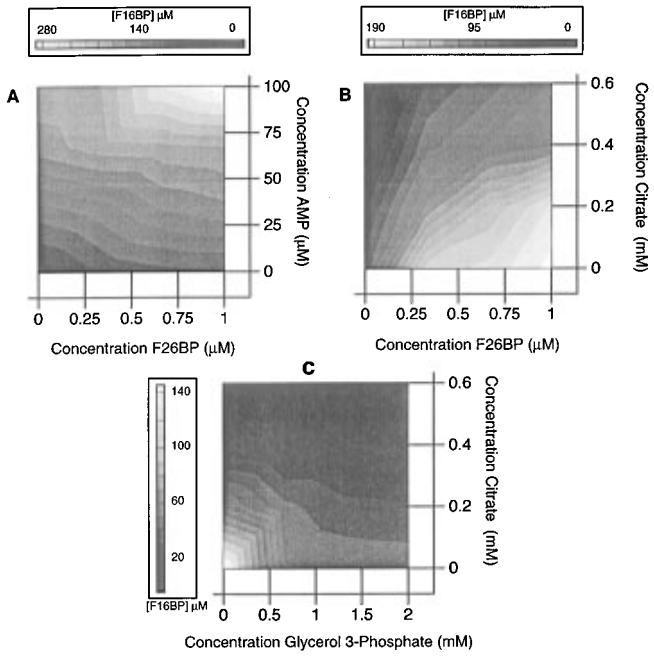

Figure 2. Experimentally determined plots of the concentration of F16BP *versus* the concentrations of effectors: (A) AMP and F26BP, (B) citrate and F26BP, (C) citrate and G3P. Black is the lowest concentration of F16BP in each graph, and white is the highest (see the shaded quantitative scale next to each plot).

After the first sample (with no effectors) is taken, we switch the inlet tube to one of the mixtures of effectors, and after 30 min take a sample of the outflow, and switch the inlet tube to the next effector mixture, and so on. After we have made about eight measurements in this way, we return the inlet tube to the enzyme buffer, wait 30 min, and sample, and then an experimental series is complete.

Measurements are taken for each effector species at a high concentration, at zero concentration, at two evenly spaced intermediate concentrations, and at all combinations of these for the two effectors, making a 4 $\times$ 4 concentration grid with 16 measured points (see Figure 2). As stated earlier, we cannot complete all of the measurements for a surface with one set of enzymes, so we must standardize between batches. Since extremely small, and therefore difficult to measure, quantities of enzyme are used, small fluctuations in activity between batches can be expected and were observed. Since each series had a measurement with only the enzyme buffer and no effectors, we used these to relate series. To make this correction, we simply multiplied the measured concentrations of F16BP in the second series by the ratio $[F16BP_1]/[F16BP_2]$, where $[F16BP_1]$ is the concentration of F16BP measured in the first sample of the first series, and $[F16BP_2]$ is the concentration of F16BP measured in the first sample of the second series.

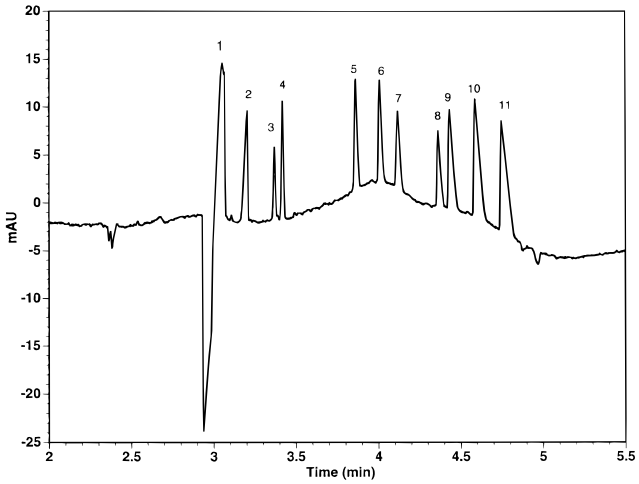

Figure 3. Electropherogram, plotted as relative light intensity at detector (in mAU) *versus* time, of 11 glycolytic metabolites using indirect UV absorbance detection. Instrument: HP ^{3D}CE; capillary, fused silica, *L* (total length) = 48 cm, *l* (length to detector) = 40 cm, 50 μm i.d.; electrolyte, 5 mM 4-hydroxybenzoate, 0.5 mM OFM Anion-BT, pH 11.6; voltage: −17 kV; current, 17.6 μA; detection, photodiode array, 280 nm; injection, 0.75 psi 5 s. Peak identification: 1 = phosphenol pyruvate (PEP) (50 μM), 2 = inorganic phosphate (45 μM), 3 = F16BP (30 μM), 4 = F16BP (40 μM), 5 = dihydroxyacetone phosphate (DHAP) (45 μM), 6 = glyceraldehyde phosphate (GAP) (45 μM), 7 = pyruvate (100 μM), 8 = F6P (45 μM), 9 = G6P (70 μM), 10 = lactate (220 μM), and 11 = AMP (190 μM). (Reproduced from Shen *et al*., 1996).

Results

As shown in Figure 3, the measurement technique used here allows for the separation and quantification of 11 major glycolytic metabolites. In this work we focus on the concentration of F16BP, and thus the most important separation is that between F16BP and F26BP. These peaks are fully base line resolved at the concentrations used in our experiment.

In order to investigate the stationary state kinetics of the F6P/F16BP cycle, we have chosen to study four effectors, two of which generally promote glycolysis (AMP and F26BP) and two of which generally inhibit glycolysis (citrate and glycerol 3-phosphate). These four species are significant effectors which convey information from a number of different systems to this metabolic regulatory point. We are interested in measuring the stationary states in the presence of three different combinations of the effectors: two glycolysis inhibitors, an activator and an inhibitor, and two activators.

Figure 2 shows the results of the three different experiments. The concentrations of effectors are plotted on the *x*- and *y*-axis, and the corrected concentration of F16BP is represented by the shade of gray.

In Figure 2A, we have plotted [F16BP] *versus* [AMP] and [F26BP]. The surface rises most steeply toward high concentrations of each effector and is fairly flat in the region of low F26BP, high AMP. Figure 2B shows [F16BP] plotted *versus* [F26BP] and [citrate]. Here the shape of the surface is similar to that shown in Figure 2A, but is rotated 45°. Figure 2C shows [F16BP] *versus* [citrate] and [glycerol 3-phosphate]. This shows the steepest transition, as the only region where there is significant conversion of F6P to F16BP is located where neither inhibitor is present.

The concentration changes along the *x*-axes in Figures 2A,B and the *y*-axes in Figures 2B,C are not as similar as one would expect, since these are essentially identical experiments (*i.e*., in Figures 2A,B the *x* axis is F26BP with none of the other effectors present). This is due largely to variations in the experimental conditions and differences in graphing range. The two experiments with citrate as an inhibitor have different starting levels of F16BPase (*i.e*., 0.2 units for Figures 2A,B *versus* 0.15 units for Figure 2C) in order to allow visualization of the inhibition effect in Figure 2C. Because starting levels of F16BP are so low in Figure 2B, one does not observe significant regulation by citrate in the absence of F26BP in Figure 2B, but one does in Figure 2C.

In Figures 2A,B, however, starting conditions were the same within the limit of the method used. In Figure 2A there was less conversion of F6P to F16BP in the absence of regulation than in Figure 2B (the steady-state concentration of F16BP in the absence of regulators was about 25 μM in Figure 2A and 60 μM in Figure 2B). This indicates that enzyme batches were not identical. This is most likely because a different stock of the enzyme F16BPase (which was not frozen along with the other enzymes, but was refrigerated in solution) was used for Figure 2A than was used for Figures 2B,C (the latter two used the same stock). It is most likely that some of the enzyme used in Figure 2B had degraded by the time of the experiment, and so the amount of enzyme used was actually less than the intended 0.2 units, whereas in Figure 2A new stock was used, and apparently it was more active. We did not compare the activity of the different enzymes before use.

An even more significant reason for the difference in the surfaces Figures 2A,B is simply that the range between low values and high ones in Figure 2A is significantly greater than that in Figure 2B. Thus, while almost no change is seen on the graph between 0 and 1 μM F26BP because of the scale used, in fact the concentration of F16BP changed by a factor of 2.5, compared with a factor of 3.1 for Figure 2B. Thus, the results are more self-consistent than they appear in Figure 2.

Numerical Model of the F6P/F16BP System. Simulations were run on a DECstation 3100 using a FORTRAN NAG routine Runge−Kutta−Merson method numerical integrator.

The effects of F16BPase under the influence of the various inputs are modeled with the rapid equilibrium random order bi−bi mechanism proposed by Liu and Frommn.[11] The influence of effectors on PFK1 is taken from a number of sources. The general form of the equation was suggested by Eschrich *et al*.[12] and updated by Arkin and Ross,[7] and includes the influence of AMP, adenosine diphosphate (ADP), ATP, F26BP, and citrate, as well as feedback from both F6P and F16BP. The influence of glycerol 3-phosphate is calculated from Figure 2 in Claus *et al*.,[13] with the assumption of noncompetitive allosteric inhibition. The effect of flow through the reactor is simulated by multiplying the difference between the input and internal concentration of F6P ($[F6P]_{in} - [F6P]_{out}$) by the flow "rate constant" (flow rate/reactor volume). The detailed sets of differential equations can be found in ref 14.

Using the constants found in the references given, we find that the effect of F26BP is underpredicted, meaning that very little change in F16BP concentration is seen upon increasing the concentration of F26BP from 0 to 1 μM. However, such concentrations of F26BP are known to exert significant regulatory effects[15,16] and clearly exert an effect in our studies. There are many possible reasons for the discrepancy. For example, the constants for the PFK1 model were determined at pH 6.6, and at high ionic strength and high phosphate and high Mg^{2+} concentrations (100 mM KCl, 20 mM K_2HPO_4, and 20 mM $MgCl_2$), whereas we used pH 7.1 and lower ionic strength, phosphate, and Mg^{2+} concentrations (50 mM KCl, 1 mM K_2HPO_4, and 5 mM $MgCl_2$). The constants for the F16BPase model were determined at pH 9.5, in a buffer containing 50 mM DTT, 100 mM KCl, and 0.05 mM nicotinamide adenine

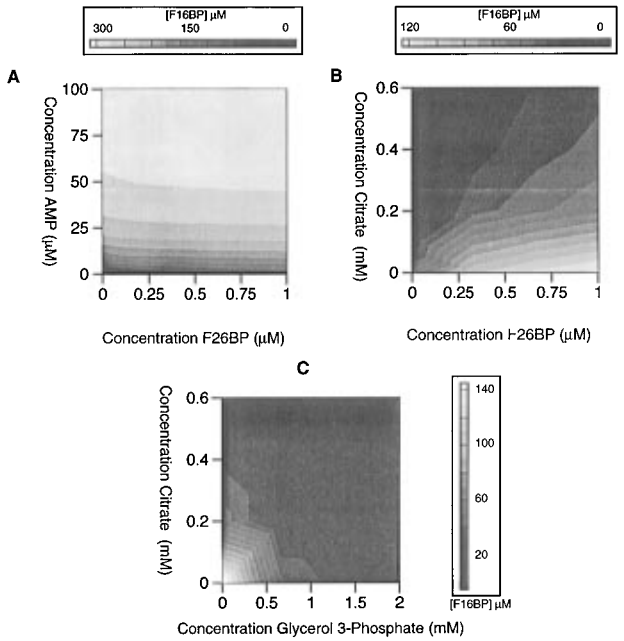

Figure 4. Numerically determined plots of the concentration of F16BP *versus* the concentrations of effectors: (A) AMP and F26BP, (B) citrate and F26BP, (C) citrate and G3P. Black is the lowest concentration of F16BP in each graph, and white is the highest.

dinucleotide phosphate. Thus, different experimental conditions are the most likely explanation for the difference between the predicted and experimentally observed effects of F26BP. To correct somewhat for this, we decrease the constants associated with F26BP in the models by a factor of 10, which brings predictions to within an order of magnitude of observations.

As discussed earlier, the enzyme activities are not the same for the three experiments. In order to simplify comparisons between model predictions and observed results, in our calculations we equate the steady-state level of F16BP in the absence of effectors with that for the given experiment. We do this by adjusting the V_{max} for PFK1, which is akin to changing its concentration. For the citrate/glycerol 3-phosphate experiment we also decrease the V_{max} for F16BPase by 25%, since this was done in the experiment.

Results of the calculations are shown in Figure 4. The agreement between experimental results and calculations is nearly quantitative when the effectors are citrate and glycerol 3-phosphate. In both cases the presence of citrate or glycerol 3-phosphate serve to turn off the production of F16BP.

The experimental and theoretical results for the F26BP and citrate surface show good qualitative agreement. Both demonstrate the hyperbolic influence of F26BP at low citrate concentrations. Both also show that citrate significantly decreases the influence of F26BP. This is an interesting case because the inputs are conflictory, and thus the results demonstrate how decisions are made in the metabolic pathway in light of conflicting signals. It may be that high concentrations of citrate indicate that the TCA cycle is saturated, and it would be of no use to the cell to expend the energy on phosphorylating F6P under those conditions. Even if the organism is well fed, not much good would come from conversion of F6P to F16BP since the glycolytic end products could not be used immediately, and so both parts of the cycle shut down (F6P production is shut down by citrate and F16BP production is shut down by F26BP). However, if citrate levels are low, then small changes in F26BP concentration have a very large effect, because blood sugar levels become the determining factor in whether to pursue glycolysis or gluconeogenesis.

The least agreement between calculations and experiment is seen for the combination of effectors AMP and F26BP. In the calculations, F26BP exerts very little influence on the steady-state concentration of F16BP at high concentrations of AMP. This is due partly to the fact that the model underpredicts the influence of F26BP in all cases, even with the correction mentioned above, but the lack of effect at high [AMP] still stands out. This effect is partially remedied if the influence of AMP is decreased by a factor of 10, so it may be that the model simply overpredicts the effect of AMP (it should also be pointed out that, at high concentrations of AMP in the calculated figure, almost all of the F6P is converted into F16BP, so the result that F26BP does not have an influence in that range may be due to the fact that no more activity on the part of the enzyme is possible). However, with this correction the experimental and theoretical graphs look quite similar only through midrange values of AMP. At high values of AMP the sharp step in the experiment at about 0.5 μM F26BP is still not predicted.

Discussion and Conclusions

If we think of the concentrations of the various effectors as inputs, and if we consider the concentration of F16BP to be a signal of whether the glycolytic pathway is "on" or "off", we can think of this cycle as a switch in the glycolytic pathway and hence a logic gate.[7] Here we briefly compare our experimental results with the calculations described in the prior work.

In Figure 2, we plot the concentration of F16BP (output) *versus* the concentrations of various effectors (inputs). Thus, the surfaces can be likened to fuzzy aggregation operators, or logic gates. In Figure 2, we are using a linear plot, rather than a log−log plot, so the transitions in the gates look much smoother than those in ref 7. Also, since we did not take measurements well past the level of saturation for an effector, or well below the level at which the effector begins to have an effect, the graphs in Figure 2 do not demonstrate the flattening at the corners of the graph which is typical of traditional logic gates.

With this in mind, our results are similar to those predicted by Arkin and Ross. Figure 2A, for example, shows the results of two activators of glycolysis. For maximal effect, both activators must be present, and despite the limited scale there is significant flattening out of the curve at low F26BP and high AMP concentrations. In the absence of effectors the concentration of F16BP is near zero. This is quite similar to the fuzzy aggregation operator for the F6P to F16BP conversion in glycolysis shown in ref 7 (in their model Arkin and Ross consider the effect of PFK2/F26BPase in addition to the enzymes discussed here). This gate may be considered a fuzzy AND operator. Figure 2B is similar in form to Figure 2A, but it is rotated by 45°. This is a F26BP NOT citrate gate, since citrate is an inhibitor of glycolysis and F26BP is an activator.

In the concentration range plotted, Figure 2C bears the strongest resemblance to a traditional logic gate, in this case a NOR gate. This is because it is "OFF" at all concentrations of citrate and glycerol 3-phosphate except when both are near zero, at which point it abruptly turns "ON". We could just as easily have plotted [F6P] and we would have an AND gate.

Instead of using [F16BP] as the output, one can consider the output to be glycolytic or gluconeogenic flux. Since we flow in only F6P, high concentrations of F16BP indicate a strong flux in the glycolytic direction. In hepatocytes, this result means that the F6P/F16BP switch in the glycolysis pathway is on. On the other hand, low concentrations of F16BP correspond to weak glycolytic flux, indicating that the switch is off. Had we wished

TABLE 1: Truth Tables for Effector Combinations

F26BP (μM)	AMP (100 μM)	output	logic gate	threshold range (μM F16BP)[a]
0	0	0		
0	1	1	OR	30−70
1	0	1		
1	1	1		
F26BP (μM)	**citrate (0.6 mM)**	**output**	**logic gate**	**threshold range (μM F16BP)**
0	0	0	F26BP	
0	1	0	AND	87−112
1	0	1	NOT	
1	1	0	citrate	
G3P (2 mM)	**citrate (0.6 mM)**	**output**	**logic gate**	**threshold range (μM F16BP)**
0	0	1		
0	1	0	NOR	36−134
1	0	0		
1	1	0		

[a] Threshold range is defined as the range of concentrations of F16BP which can serve as a threshold between 0 and 1 states for the output. The logic gate assigned is that gate which gives the largest threshold range which holds for both experiment and calculation. Since the enzyme activities are not the same, overlap in the threshold range between gates should not be considered significant.

to pursue flux as the output rather than F16BP concentration, we could have input both F16BP and F6P. We would then have concerned ourselves with whether F16BP (or F6P) was being consumed or produced. Had we looked at rates of consumption or production, we would expect the surfaces to resemble fuzzy logic aggregation operators, whereas if we had looked simply at direction of flux, our system would have been a Boolean one, and we would have expected the gates to resemble conventional digital logic gates.

We can also get a sense for the logical characteristics of the surfaces by considering threshold phenomena. If we set the threshold concentration of F16BP (output) arbitrarily, we can ask what boolean logic function does the surface describe. In Table 1 we list the logic functions of the different gates, along with the range of threshold values of [F16BP] for which the related truth tables hold for both experiment and calculations. If the concentration of F16BP is above the upper value in the threshold range, the gate is on, whereas if it is below the lower value, the gate is off. The gate described by each surface is that function for which the range of threshold values is the greatest. For example, we call the F26BP/citrate surface an F26BP AND NOT citrate gate because that is the logical function given by both experiments and calculations if the threshold range of [F16BP] is between 87 and 112 μM. However, if the treshold were between 35 and 50 μM, the surface would be an F26BP OR NOT citrate gate.

It may be useful to analyze parts of the reaction mechanism in a similar manner to electronic components, as done here, and then study composites of such parts as in electronic circuit theory. We expect such analysis to help determine the issue of function and control.

Appendix

Effect of High Concentrations of Citrate on Fructose 1,6-Bisphosphatase. Prior to carrying out our main experiments, we looked experimentally at the response of the enzymes PFK1 and F16BPase to the effectors citrate, AMP, F26BP, and glycerol 3-phosphate. We found that the observed kinetics were similar to prior predictions in all cases except one. At high concentrations, citrate actually inhibits the enzyme F16BPase, as shown in Figure 5. However, at the more physiological concentrations we use in our work (<1 mM), the effect of citrate on F16BPase appears to be negligible, though slightly inhibitory.

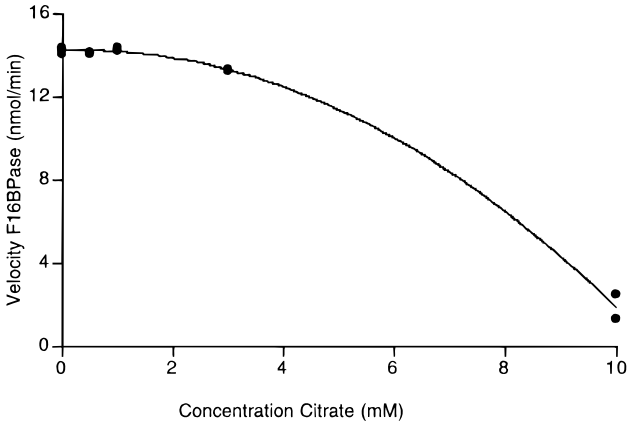

Figure 5. The velocity of the reaction *versus* the concentration of citrate. Citrate exerts very little inhibitory influence on the enzyme until it is present in nonphysiologic concentrations. The line shown is a simple quadratic fit.

This is in contrast to statements in literature, found in secondary sources such as textbooks, that citrate is an activator of F16BPase.[15,16] After an extensive search, we were unable to find evidence for this claim in the primary literature. In 1983, Hers and Hue stated: "Except for histidine, no naturally occurring positive effector of the enzyme is known."[17] Also, in his paper on the molecular physiology of citrate in metabolism, Srere mentions PFK1 in a list of enzymes affected by citrate, but not F16BPase.[18] The effect shown here may be due to the interaction of citrate with Mg^{2+} ions which is required for the function of F16BPase.[19]

Acknowledgment. We thank Dr. Peter Oefner for many helpful discussions and for the use of his experimental instruments. This work was supported in part by the National Science Foundation and the Department of Energy, Basic Energy Sciences/Engineering Program.

References and Notes

(1) Hjelmfelt, A.; Weinberger, E. D.; Ross, J. *Proc. Natl. Acad. Sci. U.S.A.* **1991**, *88*, 10983.
(2) Hjelmfelt, A.; Weinberger, E. D.; Ross, J. *Proc. Natl. Acad. Sci. U.S.A.* **1992**, *89*, 383.
(3) Hjelmfelt, A.; Ross, J. *Proc. Natl. Acad. Sci. U.S.A.* **1992**, *89*, 388.
(4) Hjelmfelt, A.; Schneider, F. W.; Ross, J. *Science* **1993**, *260*, 335.
(5) Hjelmfelt, A.; Ross, J. *Proc. Natl. Acad. Sci. U.S.A.* **1994**, *91*, 63.
(6) Laplante, J.-P.; Pemberton, M.; Hjelmfelt, A.; Ross, J. *J. Phys. Chem.* **1995**, *99*, 10063.
(7) Arkin, A. P.; Ross, J. *Biophys. J.* **1994**, *67*, 560.
(8) Zeyer, K.-P.; Dechert, G.; Hohmann, W.; Blittersdorf, R.; Schneider, F. W. Z. *Naturforsch.* **1994**, *49a*, 953.
(9) Toth, A.; Showalter, K. *J. Chem. Phys.* **1995**, *103*, 2058.
(10) Shen, P.; Hauri, D. C.; Ross, J.; Oefner, P. J. *J. Capillary Electrophor.* **1996**, *3*, 155.
(11) Liu, F.; Fromm, H. J. *J. Biol. Chem.* **1990**, *265*, 7401.
(12) Eschrich, K.; Schellenberger, W.; Hofmann, E. *Eur. J. Biochem.* **1990**, *188*, 697.
(13) Claus, T. H.; Schlumpf, J. R.; El-Maghrabi, M. R.; Pilkis, S. J. *J. Biol. Chem.* **1982**, *257*, 7541.
(14) Hauri, D. C. Ph. D Thesis, Stanford University, Stanford, CA, 1996.
(15) Stryer, L. *Biochemistry*; Freeman: New York, 1988.
(16) Voet, D.; Voet, J. G. *Biochemistry*; John Wiley & Sons, Inc: New York, 1995.
(17) Hers, H. G.; Hue, L. *Ann. Rev. Biochem.* **1983**, *52*, 617.
(18) Srere, P. A. In *Current Topics in Cellular Regulation*; Academic Press: San Diego, 1992; pp 261−274.
(19) Kwack, H.; Veech, R. L. In *Current Topics in Cellular Regulation*; Academic Press: San Diego, 1992; pp 185−207.